

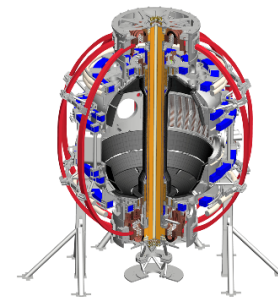


# Initial error field correction studies in the National Spherical Torus Experiment Upgrade

**Clayton E. Myers**<sup>1</sup>, S. P. Gerhardt<sup>1</sup>, J. E. Menard<sup>1</sup>, N. M. Ferraro<sup>1</sup>, J.-K. Park<sup>1</sup>,  
R. E. Bell<sup>1</sup>, B. P. LeBlanc<sup>1</sup>, M. Podestà<sup>1</sup>, and S. A. Sabbagh<sup>2</sup>

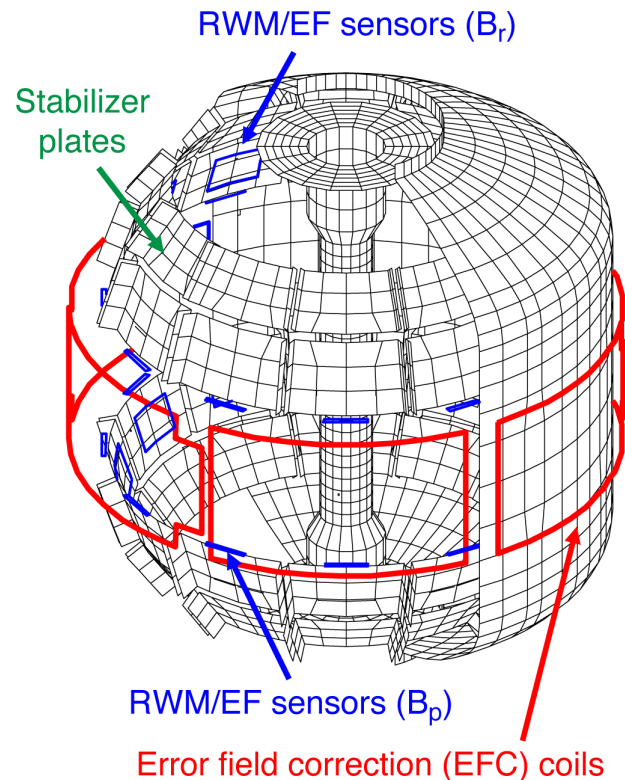
<sup>1</sup>*Princeton Plasma Physics Laboratory*, <sup>2</sup>*Columbia University*

APS-DPP 2016  
San Jose, California  
November 1, 2016



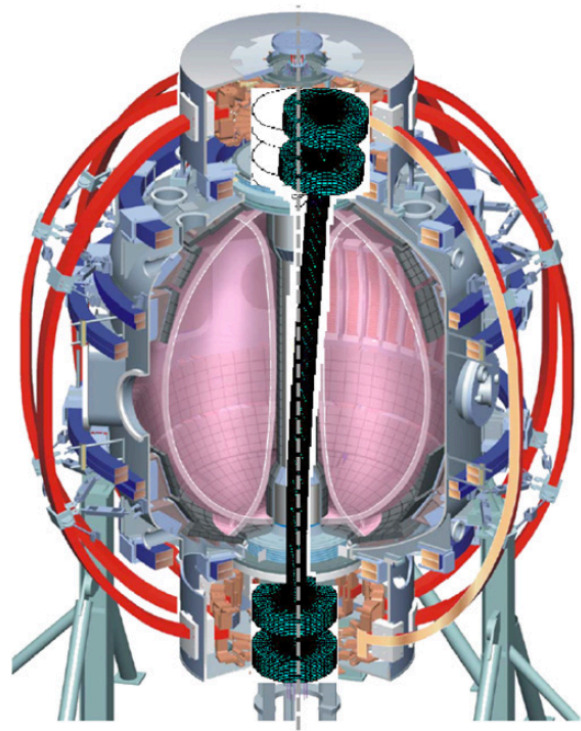
# Error field correction is key to achieving high performance

- Error field correction (EFC) objectives:
  - Probe the plasma response to applied 3D fields
  - Near-term empirical EFC prescription
  - Error field source identification
- EFC sensors and actuators in NSTX-U:
  - Four sets of 3D magnetic field sensors with 12 toroidal locations each ( $B_p/B_R$ , Upper/Lower)
  - Six midplane EFC coils to apply  $n=1,2,3$  fields simultaneously ← new capability for NSTX-U



# Candidate error field sources in NSTX-U

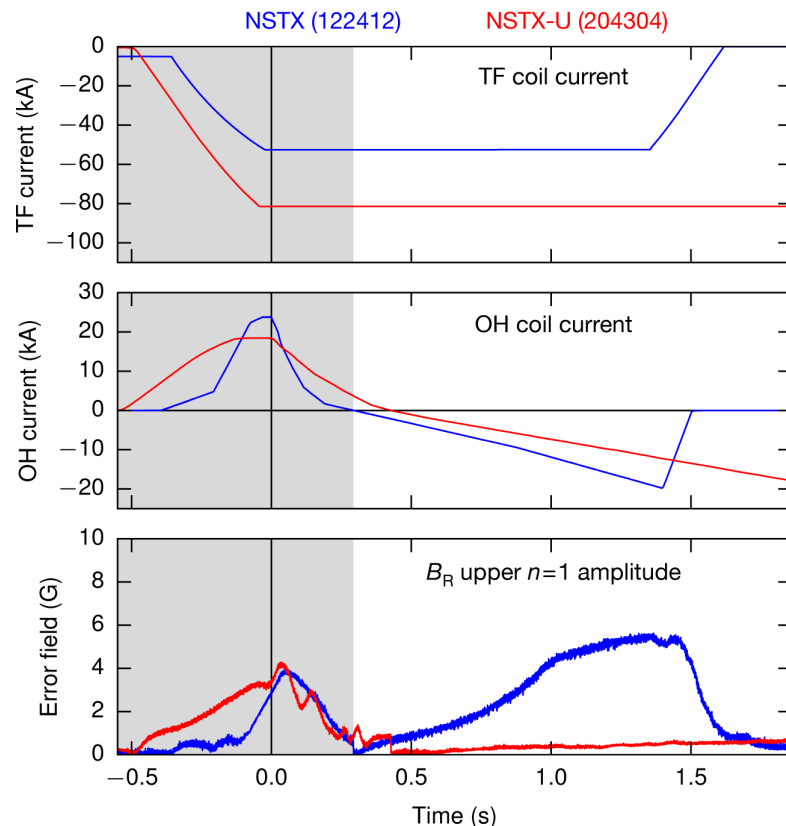
- Candidate error field sources:
  - Non-circularity of the main vertical field coil (PF5)
  - Non-axisymmetry of vessel eddy currents
  - Tilt of the TF coil from the vertical
  - Tilt of the OH coil from the vertical
  - Time-dependent OH $\times$ TF interaction [see right]
- Error field identification techniques:
  - Plasma-like vacuum shots
  - Feed-forward EFC coil currents
  - Compass scans ( $n=1$ )



Menard et al. *Nucl. Fusion* 2010

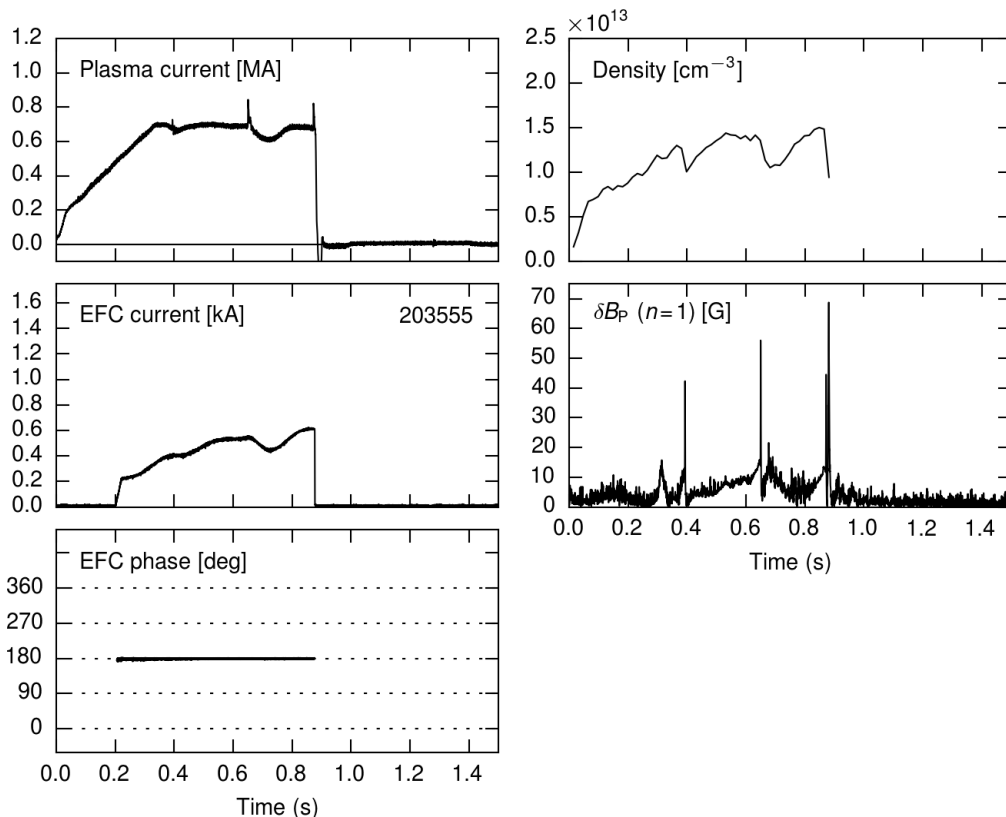
# OH×TF interaction definitively ruled out

- In NSTX, time-dependent OH×TF error field due to OH lead geometry
- Designed out of NSTX-U with coaxial OH lead assembly [Menard NF 2012]
- Compare plasma-like vacuum shots:
  - In NSTX, OH×TF error field visible in  $\delta B_R$  as  $I_{OH}$  swings negative
  - In NSTX-U, no such OH×TF error field is measured



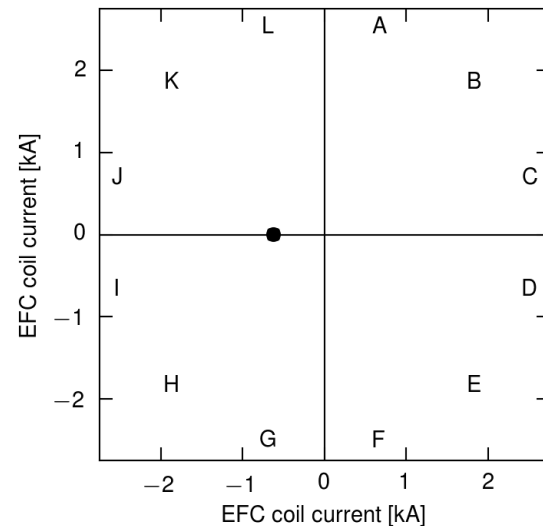
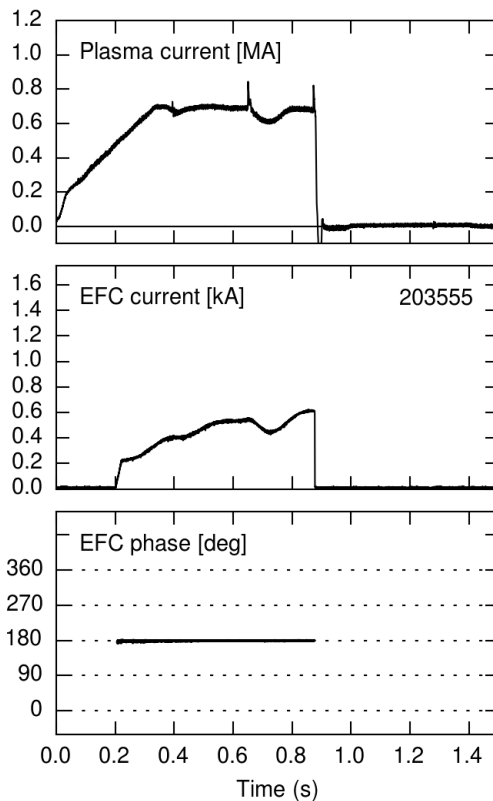
# Seek initial $n=1$ EFC with PF5-proportional 3D fields

- Apply  $n=1$  fields at fixed phase
- Set amplitude proportional to the main vertical field (PF5)
- Locking events visible in the density and in  $\delta B_p$



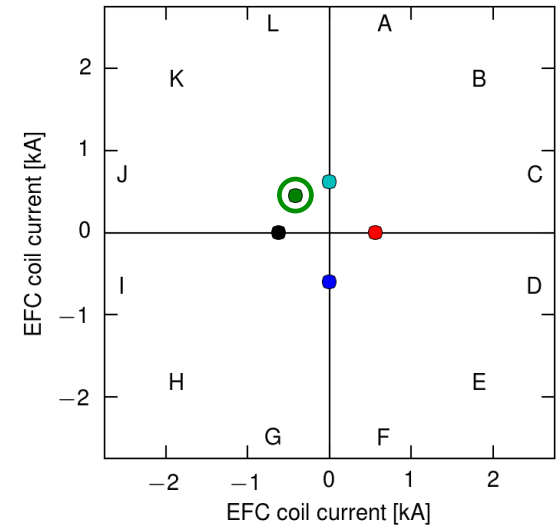
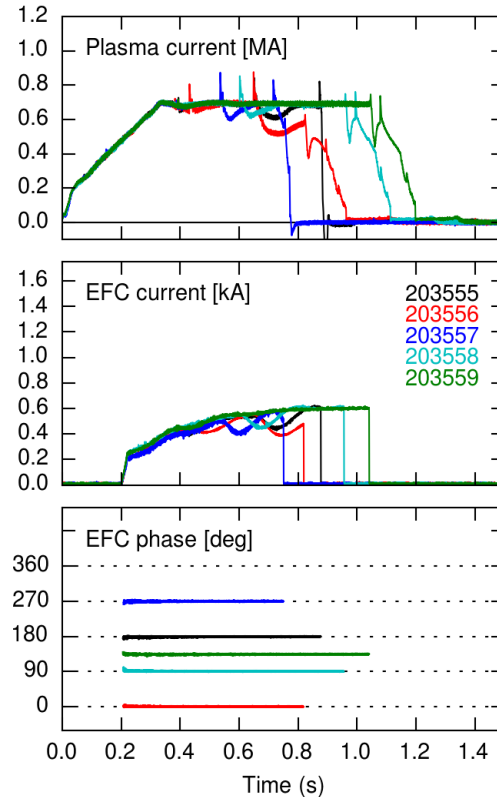
# Seek initial $n=1$ EFC with PF5-proportional 3D fields

- Apply  $n=1$  fields at fixed phase
- Set amplitude proportional to the main vertical field (PF5)
- Locking events visible in the density and in  $\delta B_p$



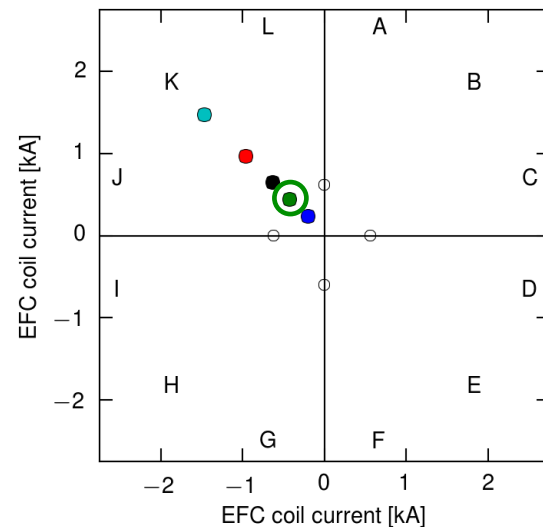
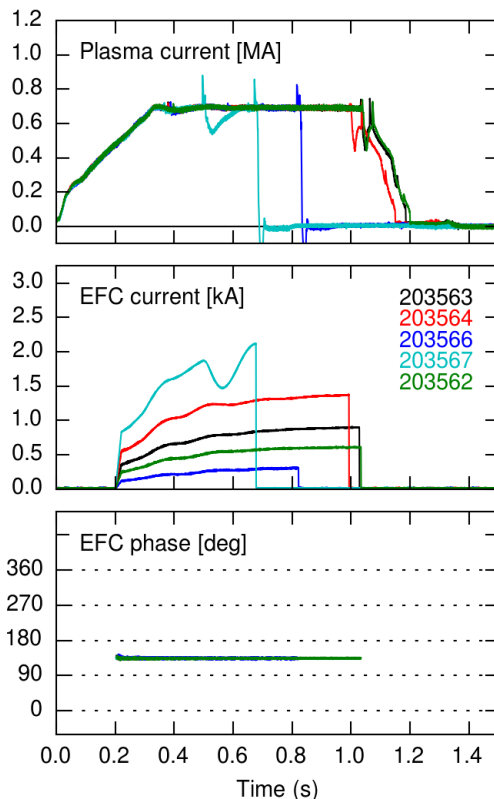
# Feed-forward phase scan: $\phi = 135^\circ$

- Apply  $n=1$  fields at fixed phase
- Set amplitude proportional to the main vertical field (PF5)
- Locking events visible in the density and in  $\delta B_p$
- Applied field phase scan:
  - Optimum phase =  $135^\circ$



# Feed-forward amplitude scan: $I_{EFC} = 600$ A

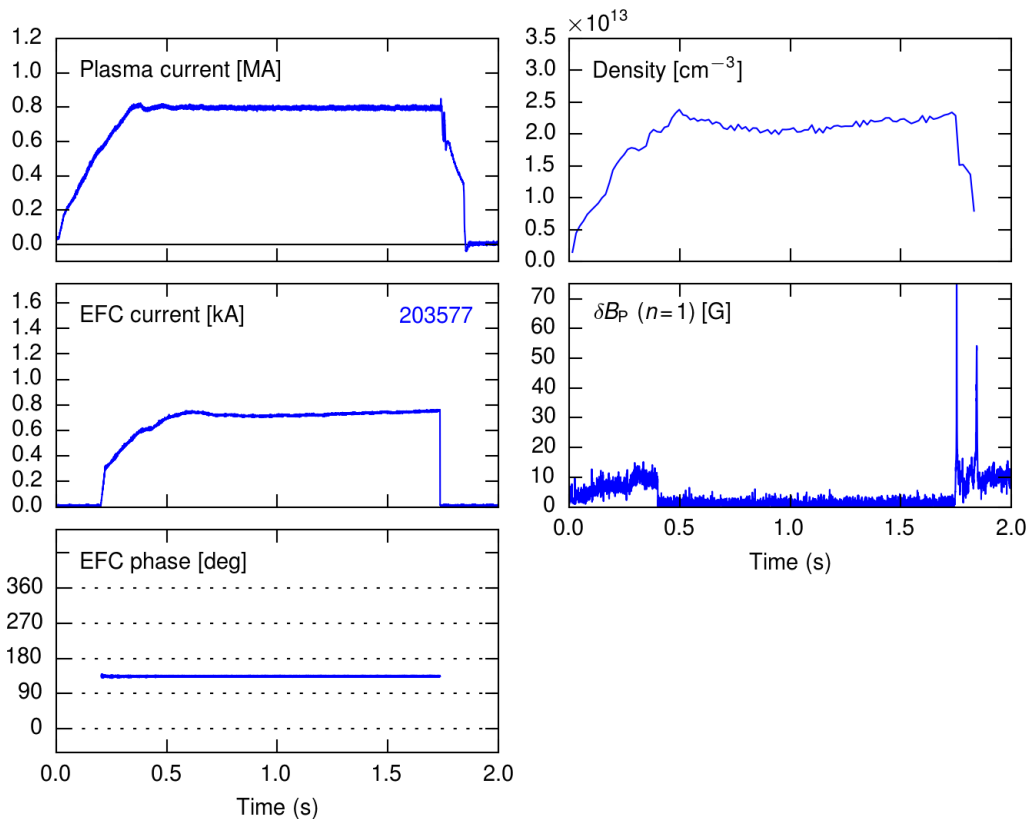
- Apply  $n=1$  fields at fixed phase
- Set amplitude proportional to the main vertical field (PF5)
- Locking events visible in the density and in  $\delta B_p$
- Applied field phase scan:
  - Optimum phase =  $135^\circ$
- Applied field amplitude scan:
  - Optimum amplitude = 600 A
  - Proportional to PF5





# Long-pulse L-mode scenario established after implementing PF5-proportional EFC

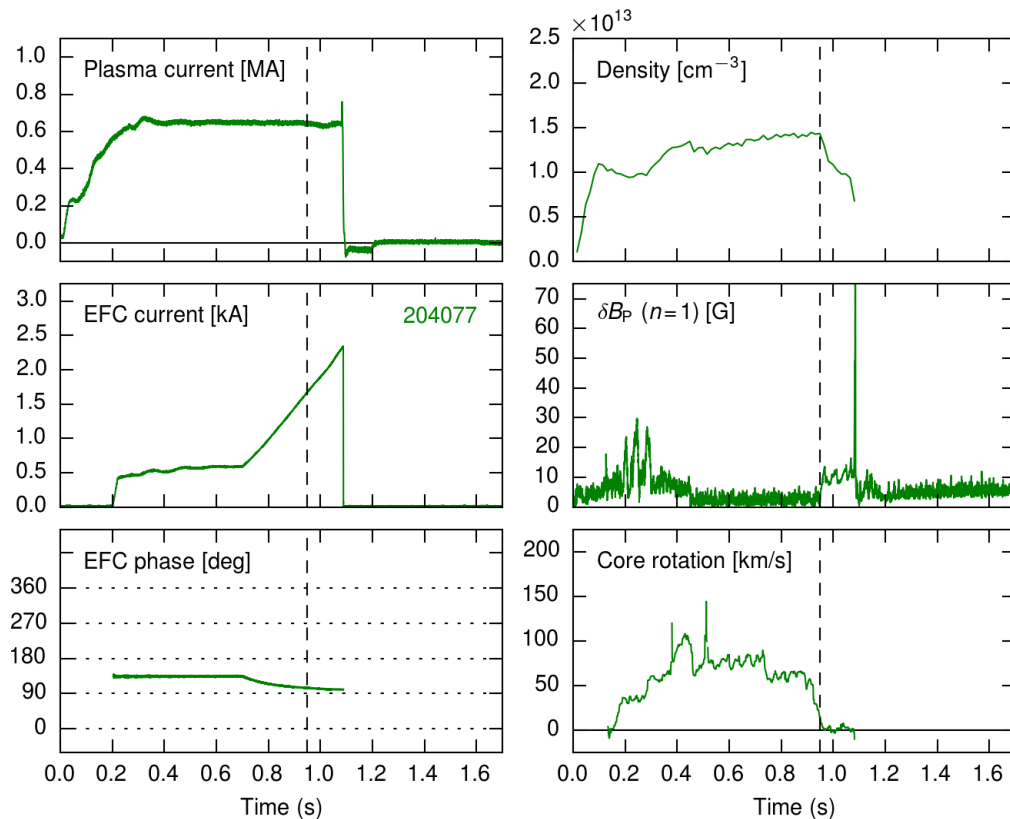
- Quickly established a robust 1 MW beam-heated L-mode scenario
- $I_p = 800$  kA with flat density evolution and quiescent  $\delta B_p$
- The discharge terminates at  $\sim 1.7$  sec due  $I_{OH}$  limit



# Refine optimum EFC with an $n=1$ compass scan

Compass scan steps:

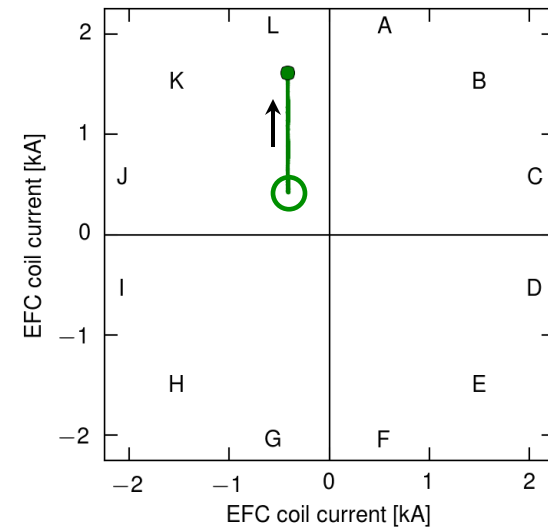
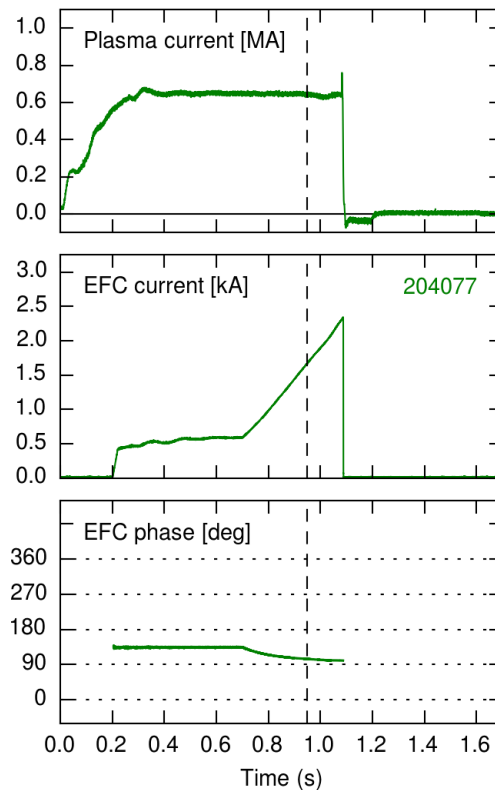
1. Select  $n=1$  phase
2. Ramp  $n=1$  amplitude until the discharge terminates



# Refine optimum EFC with an $n=1$ compass scan

Compass scan steps:

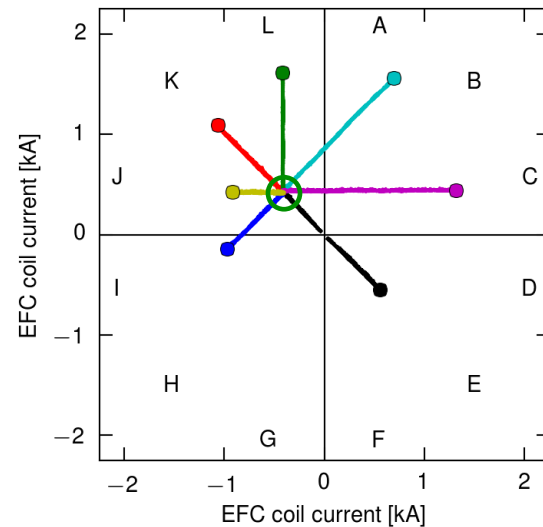
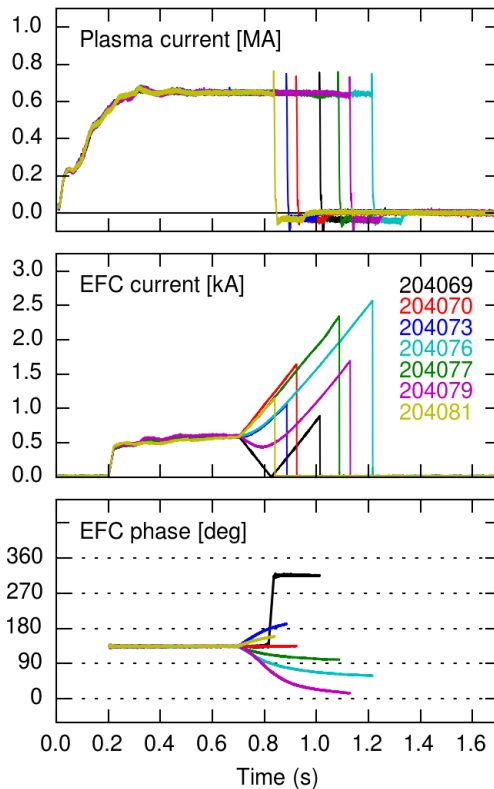
1. Select  $n=1$  phase
2. Ramp  $n=1$  amplitude until the discharge terminates



# Refine optimum EFC with an $n=1$ compass scan

Compass scan steps:

1. Select  $n=1$  phase
2. Ramp  $n=1$  amplitude until the discharge terminates
3. Repeat at multiple phases



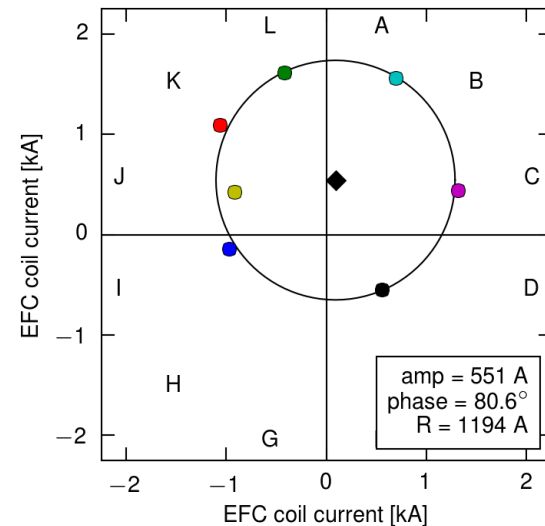
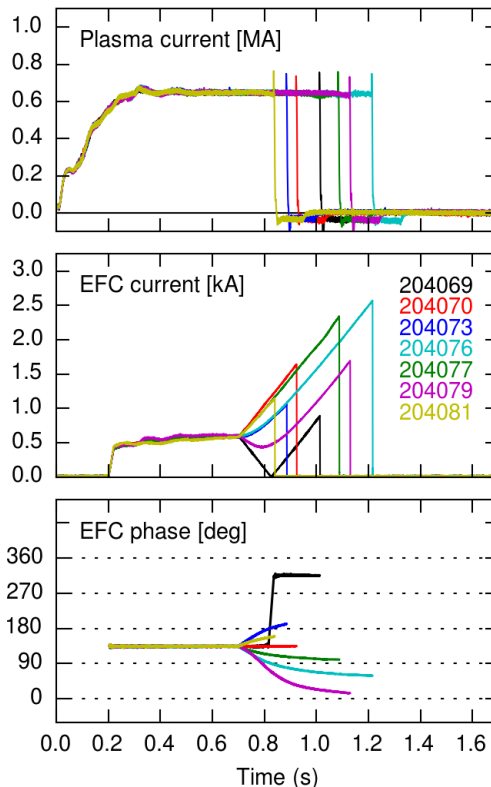
# The optimum phase shifts from $135^\circ$ to $80^\circ$

## Compass scan steps:

1. Select  $n=1$  phase
2. Ramp  $n=1$  amplitude until the discharge terminates
3. Repeat at multiple phases
4. Fit circle to locking points
5. The optimum EFC is located at the center of the circle

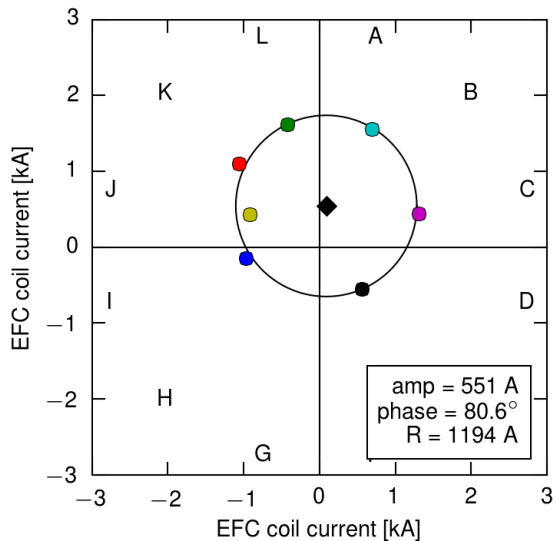
## Optimum EFC:

- $\phi = 80^\circ$  (prev.  $135^\circ$ )
- $I_{\text{EFC}} = 550 \text{ A}$  (prev.  $600 \text{ A}$ )

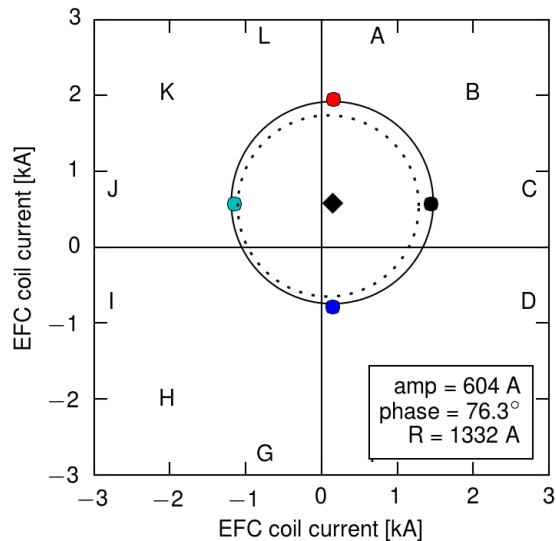


# Additional compass scans confirm the optimum EFC

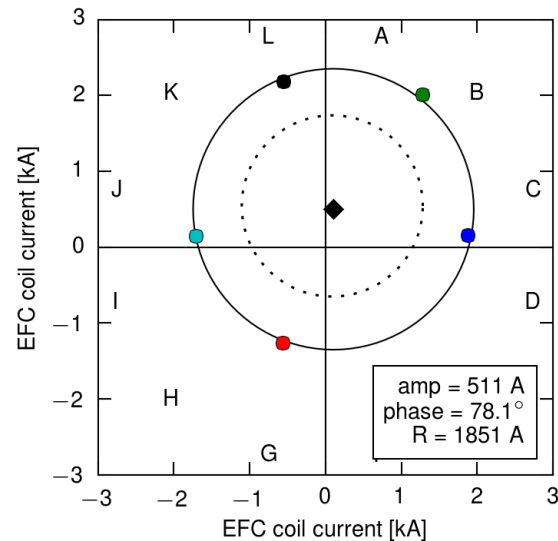
- Original compass scan
- Optimum amplitude: 550 A
- Optimum phase:  $80^\circ$



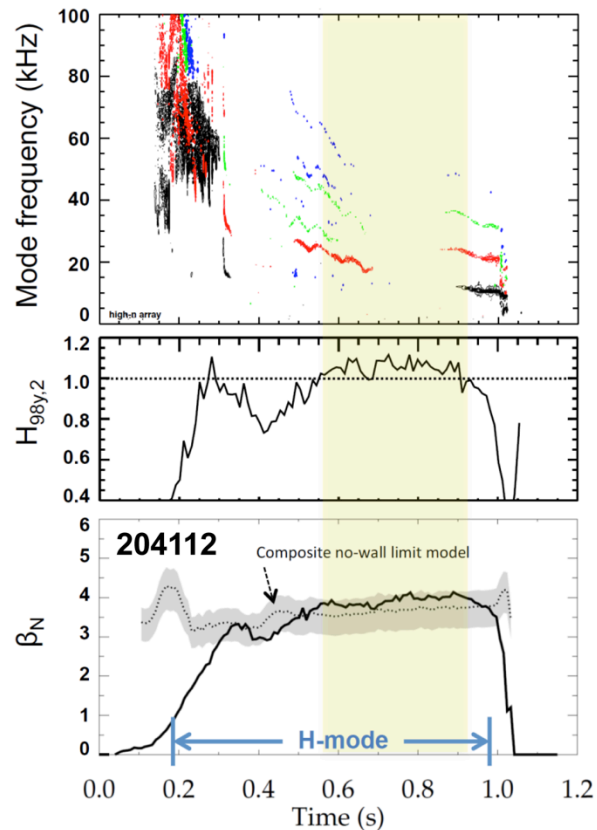
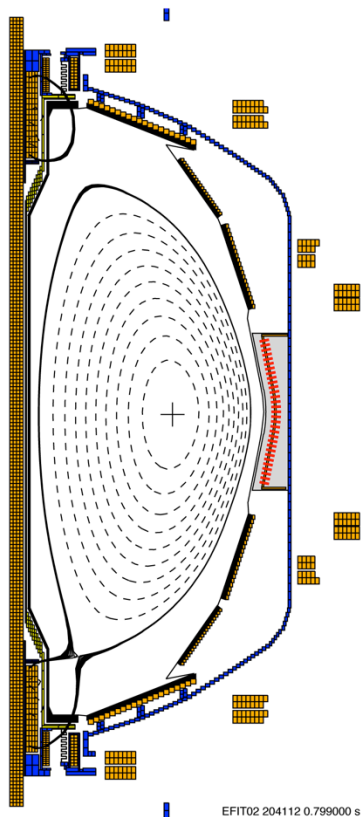
- Higher density
- Same optimum EFC
- Rotation dominates the density scaling?



- Different OH flux state
- Same optimum EFC
- Eliminates the OH as a major error field source



# High performance H-modes achieved after implementing compass-scan-optimized EFC



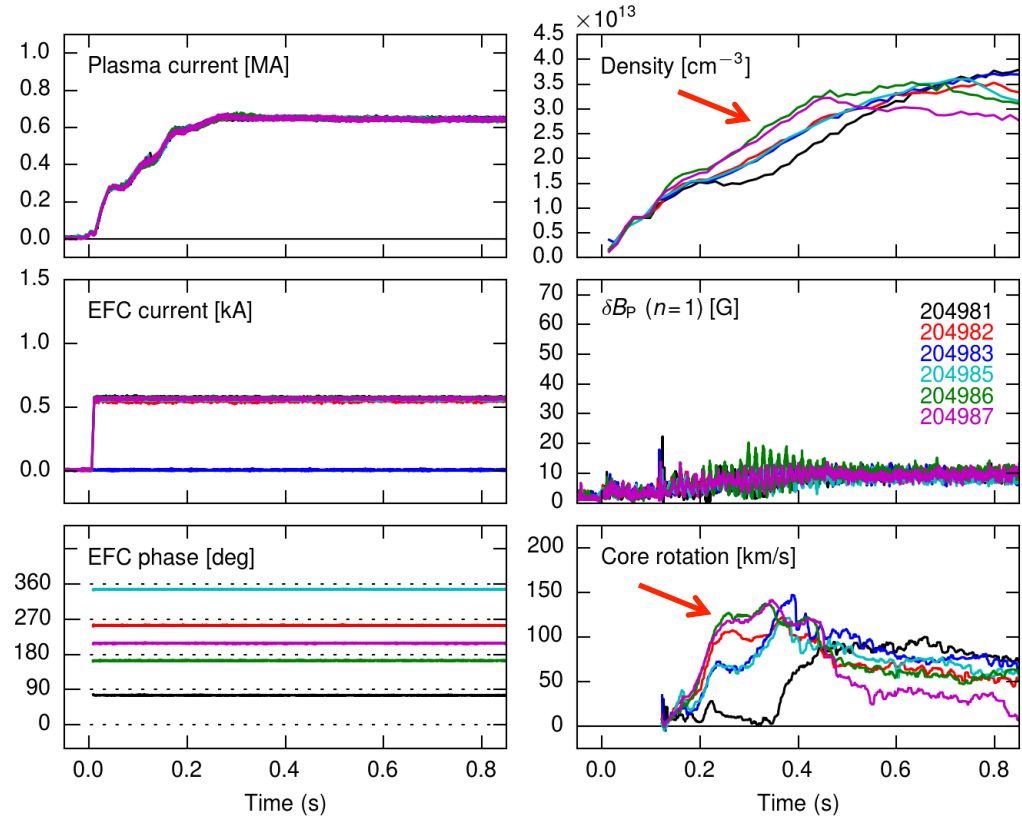
Minimal core MHD

$$H_{98y,2} \geq 1$$

$$\beta_N / \beta_{\text{no-wall}} \geq 1$$

# A different EFC phase is required early in time

- A static applied  $n=1$  phase scan early in time shows a different optimum EFC phase
- The optimum flattop phase of  $80^\circ$  is *counter-productive* early
- The phase asymmetry is visible in the density and core rotation
- Continue to search for the time-evolving error field source





# Optimized EFC enables long-pulse L-modes and high-performance H-modes in NSTX-U

- Summary:
  - Identified flattop EFC settings that enable long-pulse L-modes and high-performance H-modes
  - Eliminated two candidate error field sources:
    - OH×TF interaction
    - Tilt of the OH coil from the vertical
  - Identified an asymmetry in the optimum early time EFC with respect to the optimum flattop EFC
- More analysis and metrology are ongoing:
  - Multiple error field sources are in play (PF5 + ??)
  - Suspect a static tilt of the TF bundle is contributing
  - Time-dependent plasma response?